JTTEE5 7:213-218
©ASM International

Comparative Study of WC-Cermet Coatings Sprayed via the HVOF and the HVAF Process

L. Jacobs, M.M. Hyland, and M. De Bonte

(Submitted 13 October 1997; in revised form 6 March 1997)

The high velocity air fuel (HVAF) system is a high-velocity combustion process that uses compressed air and kerosene for combustion. Two WC-cermet powders were sprayed by the HVAF and the high-velocity oxyfuel (HVOF) processes, using an AeroSpray gun (Browning Thermal Systems Inc., Enfield, New Hampshire) and a CDS-100 gun (Sulzer Plasma Technik, Wohlen, Switzerland) respectively. Several techniques, including x-ray diffraction, scanning electron microscopy, and energy dispersive spectroscopy, were used to characterize the microstructures and phase distribution of the powders and coatings. In addition, mechanical properties such as hardness and wear resistance (pin-on-disk) were investigated. A substantial amount of W_2C was found in the HVOF coatings, as well as a high concentration of tungsten in the binder phase, indicating that oxidation and dissolution processes change the composition and microstructure from powder to coating during spraying. This was in contrast to the HVAF coatings in which composition and microstructure were unchanged from that of the powder. Additionally, the wear resistance of the HVAF coatings was superior to that of the HVOF coatings.

Keywords cemented carbides, decarburization, HVAF, HVOF, thermal spray

1. Introduction

WC-cermet coatings are generally applied using thermal spray processes including plasma spraying, detonation spraying, and high-velocity oxyfuel (HVOF) spraying. The plasma spray and HVOF methods have been well studied with respect to the microstructural characterization of the WC-cermet powders and as-sprayed coatings, as well as the investigation of their mechanical properties such as hardness and wear resistance (Ref 1-5). The main phenomena that occur during these thermal spray processes, which influence the coating performance, are the oxidation and high-temperature decomposition of tungsten carbide (WC) giving rise to the formation of di-tungsten carbide (W_2C) and a high concentration of metallic tungsten (W) dissolved in the binder phase. It has been shown that high-velocity combustion processes are particularly favorable for spraying WC-cermets, due to the high-impact velocities and the relatively low temperatures of the particles, which result in superior bond strength, hardness, and density compared to plasma sprayed WC-cermet coatings (Ref 6-8). Although a substantial improvement in coating properties is obtained when spraying WC-cermets using the HVOF process compared to the plasma spray technique, the powder still undergoes chemical and microstructural changes during HVOF spraying.

The high-velocity air fuel (HVAF) system is a high-velocity combustion spray process that uses kerosene and compressed air (not oxygen) for combustion. The HVAF system was originally developed to reduce the cost of operation, replacing pure oxygen with compressed air, and to increase the flexibility of high-velocity combustion spray processes while retaining their ability to produce superior coatings. Until now only a limited amount of research has been performed on this system, but initial studies report that coatings sprayed with the HVAF gun do not exhibit oxidation or decarburization effects that are observed in the HVOF coatings (Ref 9). There are no studies available where the same powder is deposited via the HVOF process and the HVAF process.

2. Experimental Procedure

2.1 Spray Powders

Two commercial spray powders were selected for this work. The first was a WC-10%Co-4%Cr "fused and crushed" powder, AMDRY 5843 (manufactured by Sulzer Metco). The second was a WC-12%Co CAT (carbide activation technology) powder, WC-616 (developed by Praxair Specialty Powders). Chemical and phase compositions as well as microstructures and the morphology of these two spray powders were studied. Powders were thermally sprayed onto degreased and grit-blasted substrates (No. 36 alumina grit, P = 2 atm) to a thickness of 300 μm using an HVOF and HVAF process.

2.2 HVOF Spraying

HVOF spraying was performed at the Universitat de Barcelona as part of an earlier study where the influence of spray parameters on the coating microstructure was studied (Ref 10, 11). Samples were sprayed using a CDS-100, connected to a robot arm with 6 degrees of freedom, IRB-1500 (ABB). Oxygen and propane were used as the combustion mixture. Nitrogen was used as the powder carrier gas at a flow rate of 25 slpm.

L. Jacobs and **M.M. Hyland,** The University of Auckland, Department of Chemical and Materials Engineering, Private Bag 92019 Auckland, New Zealand; and **M. De Bonte,** Katholieke Universiteit Leuven, Department of Metallurgy and Materials Engineering, de Croylaan 2, B3001 Heverlee, Belgium. Contact e-mail: l.jacobs@auckland.ac.nz.

The oxygen-to-fuel ratio was 7 to 1 (483 slpm oxygen and 63 slpm fuel). The spray distance was 200 mm.

2.3 HVAF Spraying

The samples were sprayed using an AeroSpray, Browning HVAF system. Coatings were sprayed using kerosene and air as the combustion mixture, after an initial oxygen-kerosene ignition. The spray distance was 200 mm and the chamber pressure was 400 kPa (60 psi).

2.4 Powder and Coating Characterization

The carbon content of the powders and of the coatings was determined by pyrolysis using a LECO CS-444 (LECO Corporation, MI, USA). The phase composition was investigated by x-ray diffraction (XRD) using CuK(α) radiation in the range 2θ = 30 to 110°. Characterization of the HVOF coatings was carried out as described in Ref 10 and 11 where the morphology of the powder, and the microstructure of the powder and of the metallographically polished coating cross sections, were investigated by scanning electron microscope (SEM) using secondary and backscattered electrons. The chemical composition of the material in selected areas was determined by energy-dispersive spectroscopy (EDS). The same procedure was used to characterize both the powders and the HVAF coatings. The micro and macro Vickers hardnesses were measured using loads of 0.1 and 1 kg, respectively. Sliding wear and friction experiments were conducted on a pin-on-disk apparatus (ball-on-flat) under ambient conditions (Fig. 1). The counterbody was a 10 mm diam corundum ball. The coatings were polished to a thickness of 150 µm before testing. The linear speed of the ball against the test disks was 0.46 m/s, the load was 49 N, and 20,000 revolutions were performed in each test. After 10,000 cycles, the test was stopped and the corundum ball replaced. The test was then resumed, and another 10,000 cycles were performed on the existing wear track. This test procedure induces accelerated wear. At least six tests were conducted for each material. The volume loss of the coatings was measured with a Rodenstock RM 600 laser profilometer (Feinpruf Perthen GmbH, Göttingen, Germany) and used as a measure of wear resistance.

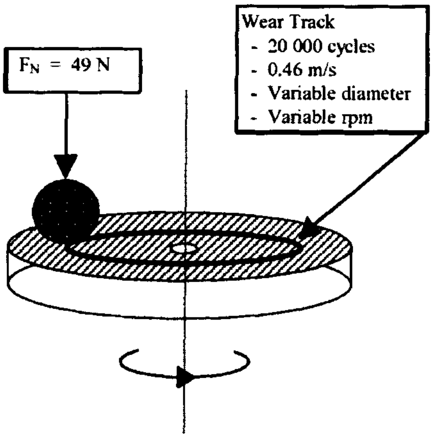

Fig. 1 Schematic presentation of the pin-on-disk apparatus

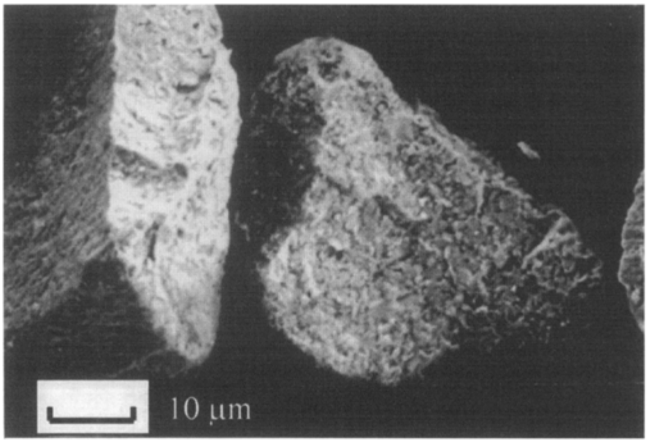

Fig. 2 SEM image (SE) showing the morphology of the "fused and crushed" WC-Co-Cr powder

3. Results and Discussion

3.1 Characterization of the Spray Powders

The powders were characterized to determine changes that take place during spraying (Table 1).

Table 1 Results of the carbon analysis and XRD analysis of the powders and the HVOF and HVAF sprayed coatings

Material	Process	% C analyzed	Main phases
WC-Co-Cr	Powder	5.3	WC,(Co,W)$_6$C
	HVOF	4.9	WC,W$_2$C
	HVAF	5.3	WC,(Co,W)$_6$C
WC-Co	Powder	5.3	WC,Co
	HVAF	5.3	WC,Co

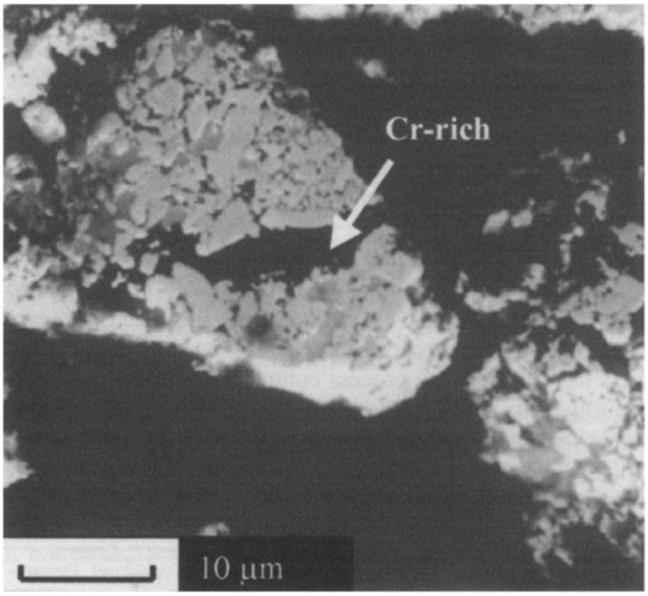

Fig. 3 SEM image (BSE) of polished cross section of WC-Co-Cr powder in which three phases can be distinguished; WC particles, a light metallic phase rich in cobalt, and a dark metallic phase rich in chromium

WC-Co-Cr Powder. The powder contained 5.31 wt% C. X-ray diffraction analysis identified WC as the main phase. The η phase $(Co,W)_6C$ was also identified, but the diffraction lines were shifted to lower lattice parameters, indicating a substitution of cobalt- atoms by chromium- atoms in the crystal structure. Also a wide, low-intensity peak was observed that coincides with the 100% diffraction line of Cr_7C_3. This powder showed the typical "fused and crushed" particle morphology. The particles have angular and blocky shapes. At higher magnification, the mostly dense, homogeneous and pore-free surfaces of the grains become apparent (Fig. 2). Scanning electron microscopy investigation of the polished cross sections shows a dense and pore-free microstructure and a homogeneous distribution of WC particles in the metallic binder phase. Backscattered electron images show a metallic binder phase with two different compositions; a cobalt-rich and a chromium-rich phase (Fig. 3).

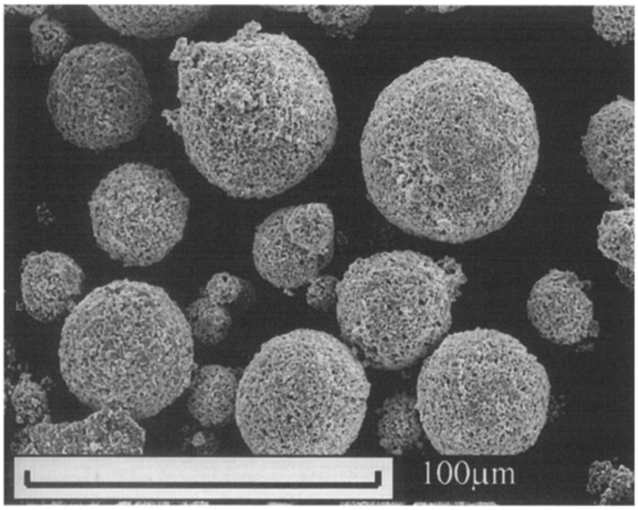

Fig. 4 SEM image (SE) showing the spherical morphology of the WC-Co powder

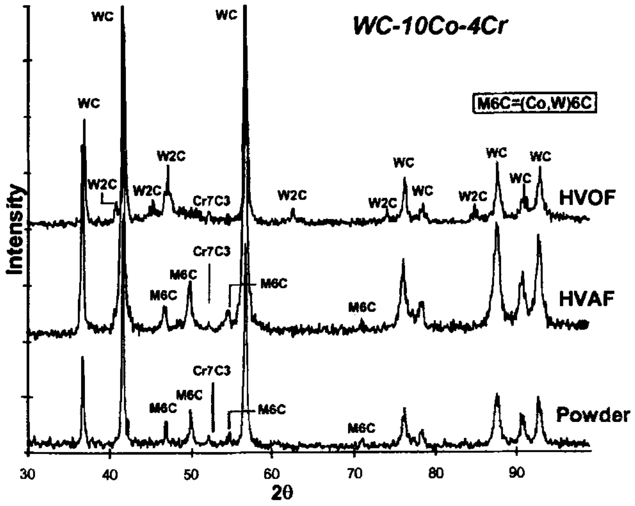

Fig. 6 XRD patterns of the WC-Co-Cr powder, HVOF, and HVAF coatings. There are no changes in the phase analysis between the powder and the HVAF coatings.

WC-Co Powder. The powder contained 5.3 wt% C. X-ray diffraction analysis identified cobalt and WC as the main phases. The particles exhibit a spherical shape (Fig. 4). Scanning electron microscopy and EDS investigation of the polished cross section show a very porous microstructure. The WC particles are evenly coated by the cobalt matrix, which results in a homogeneous dispersion of the blocky WC particles in the cobalt-binder phase (Fig. 5).

3.2 Microstructure and Chemistry of the Coatings

Strongly adherent (>80 MPa) coatings were obtained with both the HVOF and the HVAF systems. Carbon analysis shows a carbon loss of 10 wt% for the HVOF sprayed WC-Co-Cr coatings, while both the WC-Co-Cr and the WC-Co HVAF coatings retain the initial carbon content of the powder (Table 1).

Phase Analysis. The XRD patterns of the WC-Co-Cr powder and the coatings sprayed by HVAF and HVOF are compared in Fig. 6. WC-Co-Cr coatings produced by the HVOF process show the presence of the W_2C phase and disappearance of the

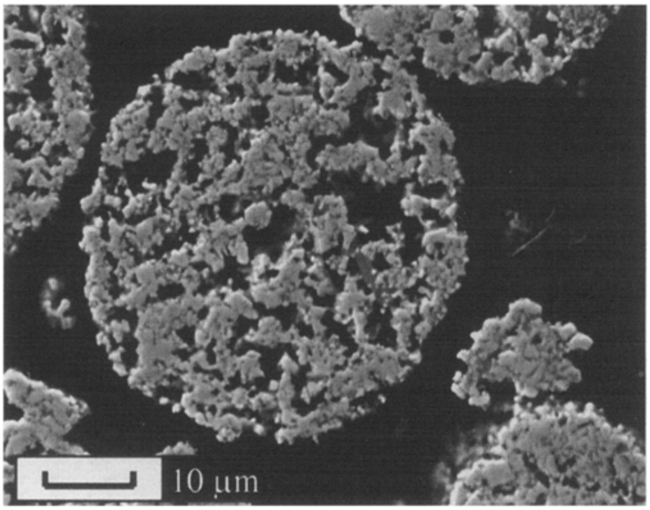

Fig. 5 SEM image (SE) of the polished cross section of the WC-Co powder showing a porous structure

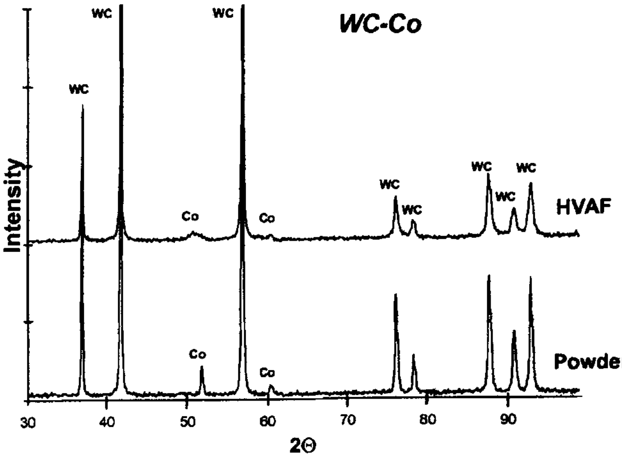

Fig. 7 XRD patterns of the WC-Co powder and HVAF coatings

(Co,W)$_6$C phase. This indicates decarburization due to high-temperature oxidation in flight. Thus, the WC-Co-Cr powder is subject to considerable phase transformation during HVOF spraying. This is in contrast to the WC-Co-Cr and WC-Co HVAF coatings (Fig. 7), where no significant difference between the diffraction pattern of the powder and that of the coatings could be observed. This indicates that there is no substantial decarburization or oxidation of the material during HVAF spraying of both WC-cermet powders.

Microstructure. Polished cross sections of the coatings were analyzed by SEM using backscattered electrons (BSE), thereby giving atomic number contrast. WC particles show up very bright (W is a heavy element), while the metallic matrix has different shades of gray, depending on the amount of cobalt and chromium it contains locally (cobalt and chromium are lighter elements). Energy-dispersive spectroscopy analysis verified that the gray tones in the BSE images could be used as a measure of the composition. As reported previously (Ref 10, 11), the WC-Co-Cr HVOF coatings contained blocky WC particles, somewhat rounded due to oxidation and high-temperature dissolution processes. A binder phase of varying composition was observed; light gray areas contained high percentages of tungsten, and darker areas contained high percentages of cobalt and/or chromium. The outer layers of the powder particles are more prone to oxidation and dissolution reactions during spraying, causing the matrix to be tungsten-rich in certain areas and giving the coatings a "segregated" microstructure (Fig. 8). In some areas, the WC particles have completely disappeared due to these reactions, leaving a tungsten-rich binder phase and W$_2$C dendrites behind. W$_2$C crystals could be observed as very bright halos around the WC particles and as dendrites. This phase is richer in the heavy element tungsten and, therefore, showed up brighter than the WC particle (Fig. 9). The presence of the W$_2$C phase is a further indication of the decarburization reactions that take place during spraying. Local concentrations of chromium carbides could be seen either in the form of blocky particles or as dendrites.

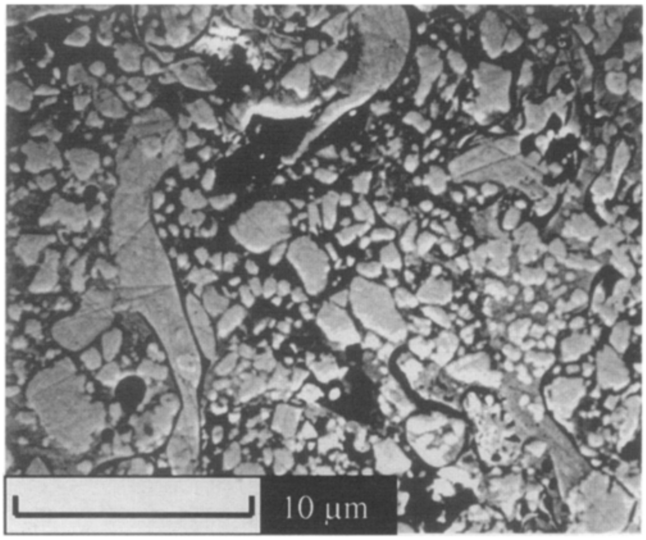

Fig. 8 SEM image of WC-Co-Cr HVOF sprayed coating (BSE). Note the blocky, somewhat rounded WC particles, some with bright W$_2$C halos around them, surrounded by gray metallic matrix of varying composition.

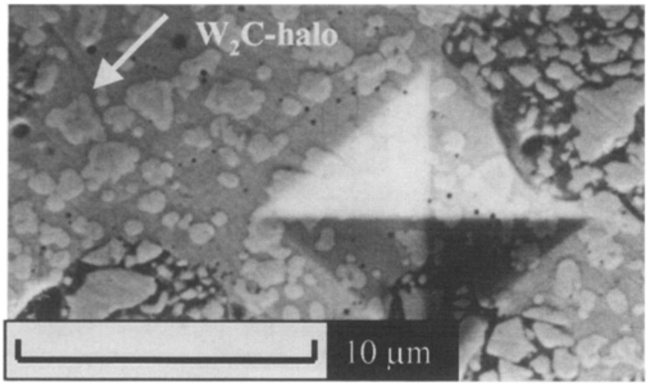

Fig. 9 SEM image of WC-Co-Cr HVOF coating (BSE). Note the W$_2$C halos around the WC particles. The binder phase is light gray, which indicates a high percentage of tungsten is present.

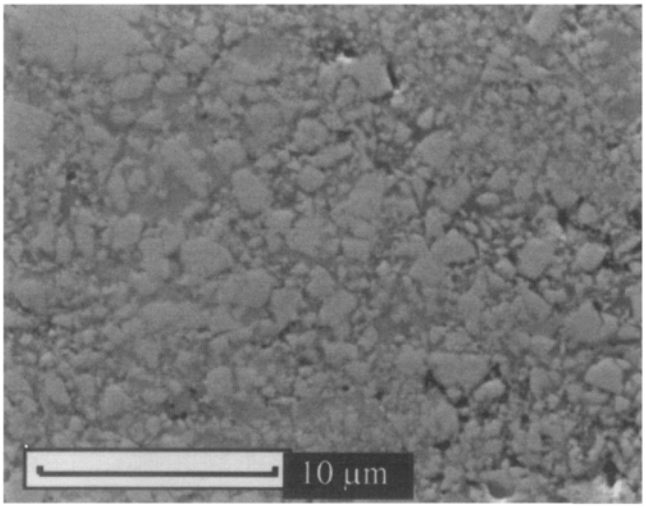

Fig. 10 SEM image of the WC-Co-Cr HVAF sprayed coating (BSE)

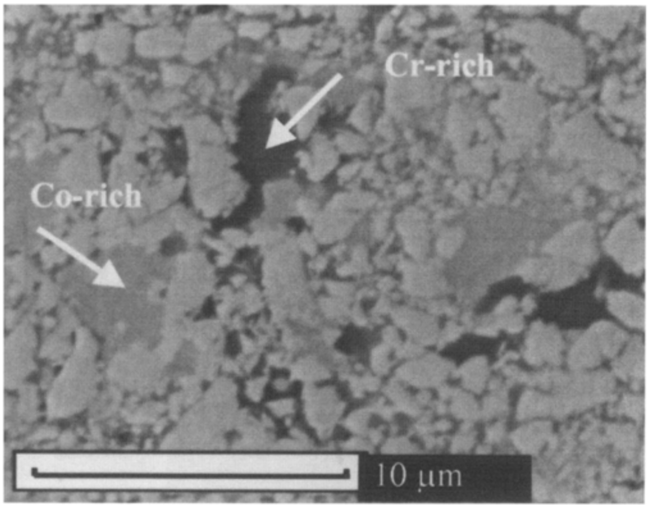

Fig. 11 SEM image (BSE) of the WC-Co-Cr HVAF sprayed coating. EDS analysis has shown that the dark areas are chromium rich, and should not be confused with porosity.

Both HVAF coatings also showed the presence of blocky WC particles whose shape was not affected by the spray process. In the case of the WC-Co-Cr coatings (Fig. 10, 11), binder phase of varying composition was observed, but again, when compared to SEM images of the powder, there was no indication that the binder phase changed composition during spraying. No chromium carbides could be visually detected using backscattered electrons. The SEM investigation of WC-Co coatings also shows the presence of an unaltered cobalt binder phase (Fig. 12). These findings confirm the XRD results.

3.3 Mechanical Properties of the Coatings

Hardness. As mentioned in the previous paragraph, the WC-Co-Cr HVOF coatings exhibit a "segregated" microstructure in which larger areas of metallic phase, with a varying tungsten content, are scattered among the finely dispersed WC particles. Therefore, in order to obtain reproducible and thus valuable microhardness results, a distinction was made between measurements made in the metallic regions and measurements made in the regions with finely dispersed carbides (Table 2). An average hardness of 1220 HV was obtained for the metallic phase, which was considerably lower than the average microhardness of the fine carbide structure of 1510 HV. The HVAF sprayed coatings did not show this segregation. There were no large areas of metallic phase detected, and thus only the microhardness of the fine carbide structure was evaluated. The WC-Co-Cr coatings had an average microhardness of 1570 HV. The WC-Co coatings showed an average microhardness of 1010 HV.

The higher macrohardness of the HVAF sprayed WC-Co-Cr coatings compared to the HVOF coatings reflects the trend exhibited by the microhardness tests. During HVAF spraying the WC particles do not disintegrate, and tungsten does not dissolve in the matrix. The initial fine structure of the WC-Co-Cr powder is thus retained and results in harder and more dispersed coatings.

Wear resistance. Wear data are shown in Table 2. The WC-Co-Cr coatings sprayed by the HVAF process have a wear resistance that is about seven times that of the HVOF-sprayed WC-Co-Cr coatings. The HVAF-sprayed WC-Co coatings exhibited a wear resistance that is about twice that of the WC-Co-Cr HVAF coatings. These findings seem to support the general belief that the presence of W_2C has a negative effect on the coating performance and that a good distribution of hard WC particles in a ductile matrix is beneficial for the wear resistance (Ref 12). The absence of W_2C together with a ductile cobalt matrix makes the WC-Co HVAF coating the best performer of the three tested coatings.

4. Conclusions

It has been demonstrated that the HVAF process does not change the chemistry or the microstructure of the investigated WC-cermet powders during spraying. No decomposition or oxidation processes take place during HVAF spraying, which results in coatings with a 100% retention of WC particles and a complete absence of W_2C. This is in contrast to the investigated HVOF process where oxidation and decomposition processes are responsible for a considerable WC loss during spraying and for the formation of the brittle W_2C phase.

The results of the mechanical tests reveal that the finer, more dispersed microstructure of the WC-Co-Cr HVAF coatings results in a higher hardness and an improved wear resistance in comparison to the HVOF sprayed WC-Co-Cr coatings. The HVAF sprayed WC-Co coatings exhibit the best wear behavior of the three tested coatings.

It has to be mentioned that the CDS-100 gun is not representative for all presently available HVOF processes. More work should be carried out, especially on HVOF guns that use oxygen and kerosene for combustion, to establish the influence of fuel, oxygen content, and temperature on the decarburization reactions.

Acknowledgment

The authors would like to thank the New Zealand Foundation for Research Science and Technology who provided the fund-

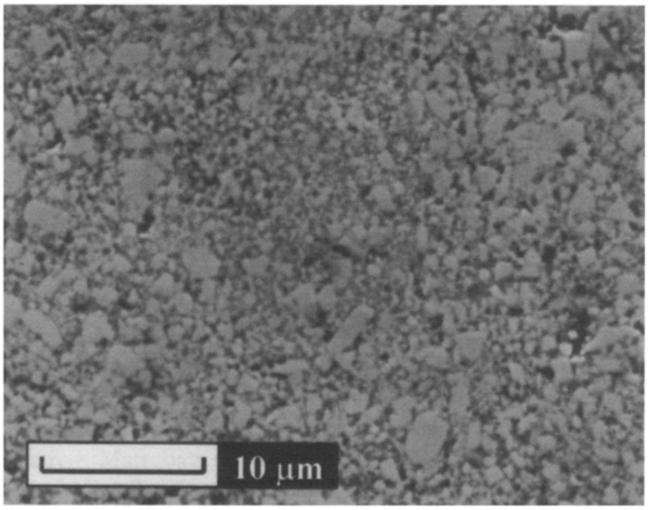

Fig. 12 SEM image (BSE) of the polished cross section of the WC-Co coating sprayed by HVAF

Table 2 Results of the hardness measurements and the pin-on-disk wear test

Powder	Process	Microhardness, HV 100 g	Macrohardness, HV 1 kg	Wear rate CSA(a), × 10^3 µm^2
WC-Co-Cr	HVOF	1220 ± 70(b) 1510 ± 100(c)	880 ± 50	3.63
	HVAF	1570 ± 70	1050 ± 60	0.53
WC-Co	HVAF	1010 ± 120	630 ± 100	0.23

(a)CSA, cross-sectional area of the wear track. (b) Hardness measured in metallic region. (c) Hardness measured in region with dispersed carbides

ing. HVAF spraying experiments were carried out at Holster Engineering, Tokoroa, New Zealand. The authors would like to thank them for providing equipment and technical support. HVOF spraying was carried out at the Universitat de Barcelona. The authors wish to acknowledge the research group of Professor Guilemany. The authors would also like to thank Praxair Specialty Powders and Sulzer-Metco for providing the spray powders.

References

1. S.F. Wayne and S. Sampath, Structure/Property Relationships in Sintered and Thermally Sprayed WC-Co, *J. Therm. Spray Technol.*, Vol 1 (No. 4), 1992, p 307-315
2. A. Karimi, Ch. Verdon, and G. Barbezat, Microstructure and Hydroabrasive Wear Behaviour of High Velocity Oxy-Fuel Thermally Sprayed WC-Co(Cr) Coatings, *Surf. Coat. Technol.*, Vol 57, 1993, p 81-89
3. L.M. Berger, P. Vuoristo, T. Mäntylä, W.Kunert, W. Lengauer, and P. Ettmayer, Structure, Properties and Potentials of WC-Co, Cr_3C_2-NiCr and TiC-Ni-Based Hardmetal-like coatings, *Therm. Spray: Practical Solutions for Engineering,* C.C. Berndt, Ed., ASM International, 1996, p 89-96
4. M.S.A. Khan and T.W. Clyne, Microstructure and Abrasion Resistance of Plasma Sprayed Cermet Coatings, *Therm. Spray: Practical Solutions for Engineering,* C.C. Berndt, Ed., ASM International, 1996, p 113-122
5. H.J. Kim, Y.G. Kweon, and R.W. Chang, Wear and Erosion Behavior of Plasma-Sprayed WC-Co Coatings, *Therm. Spray Technol.,* Vol 3 (No. 2), 1994, p 169-178
6. S.Y. Hwang, B.G. Seong, and M.C. Kin, Characterization of WC-Co Coatings using HP, HVOF Process, *Thermal Spray: Practical Solutions for Engineering,* C.C. Berndt, Ed., ASM International, 1996, p 107-112
7. L.M. Berger, P. Vuoristo, T. Mäntylä, W. Kunert, W. Lengauer, and P. Ettmayer, Microstructure and Properties of WC-Co-Cr Coatings, *Thermal Spray: Practical Solutions for Engineering,* C.C. Berndt, Ed., ASM International, 1996, p 97-106
8. H. Kreye, Characterization of Coatings Produced by High Velocity Flame Spraying, *Thermal Spray,* I.A. Bucklow, Ed., London, UK, 1989, p 24-1 to p24-9
9. K. Akimoto, K. Akimoto, and Y. Horie, Study of HVAF WC-Cermet Coatings, *Thermal Spray: Current Status and Future Trends,* A. Ohmori, Ed., High Temperature Society of Japan, 1995, p 313-316
10. J.M. Guilemany, L. Delaey, F.J. Sanchez, and L. Jacobs, Characterization of WC + Co + Cr Coatings Obtained by HVOF-Spraying, *Metall. Ital.,* Vol 88 (No. 2), 1996, p 133-136
11. L. Jacobs, "Influence of the HVOF Process Conditions on the Structure of WC-Co-Cr Coatings," Master Thesis, Katholieke Universiteit Leuven, 1995 (in Dutch)
12. J. Nerz, B. Kushner, and A. Rotolico, Microstructural Evaluation of Tungsten Carbide Cobalt Coatings, *Thermal Spray Coatings: Properties, Processes and Applications,* T.F. Bernecki, Ed., ASM International, 1991, p 115-120